Theoretical studies of the passivants' effect on the Si_xGe_{1-x} nanowires: Composition profiles, diameter, shape, and electronic properties

Xiao-Bao Yang,[1,2,3,a)] Yu-Jun Zhao,[2,3] and Hu Xu[1,b)]
[1]*Nanostructure Institute for Energy and Environmental Research, Division of Physical Sciences, South University of Science and Technology of China, Shenzhen, People's Republic of China*
[2]*Department of Physics, South China University of Technology, Guangzhou, GuangDong 510640, People's Republic of China*
[3]*State Key Laboratory of Luminescent Materials and Devices, South China University of Technology, Guangzhou 510640, People's Republic of China*

(Received 5 August 2013; accepted 30 September 2013; published online 18 October 2013)

Theoretically, we have performed a systematic investigation on the passivants' effect on the geometrical and electronic properties of Si_xGe_{1-x} nanowires. First-principles calculations revealed that, in the nanowires passivated by fluorine (F)/chlorine (Cl)/hydrogen (H) atoms, Si atoms preferred to segregate towards the surface due to the stronger Si–X bonds than that of Ge–X bonds (X = F, Cl, H). The energy barriers of X atoms' desorption is higher than that of the Si/Ge atoms' exchanging, inducing a feasible and strong surface segregation of Si atoms at proper temperature. Considering the Si/Ge interactions and mixing entropy, the composition profiles of Si/Ge distributions are obtained by minimizing the Gibbs free energy, which indicates the outmost layer of surface should be mostly occupied by Si. With total Si surface segregation, the diameter and shape of most stable Si_xGe_{1-x} nanowires are found to be determined by the composition x and the passivants' chemical potential. In addition, charge distribution of near-gap levels can be modulated through the surface passivants. Our finding provides a practical avenue to tune the electronic properties of Si_xGe_{1-x} nanowires, by modulating the morphologies of nanowires with the composition control of Si/Ge and the chemical potential of passivants. © *2013 AIP Publishing LLC*. [http://dx.doi.org/10.1063/1.4825196]

I. INTRODUCTION

The indirect bandgap limits the Si and Ge applications in optoelectronics due to the weak light emission, while Si_xGe_{1-x} ($0 < x < 1$) alloys and films offer a continuously variable system with tunable electronic and optical properties. By controlling the growth of superstructures on the Si_xGe_{1-x} film, theoretical studies showed that Si and Ge can be spatially melded together into one strongly dipole-allowed direct-gap material.[1] Si_xGe_{1-x} nanowires, including the core-shell structures,[2] have been demonstrated as novel electronic, photovoltaic, optoelectronic, and low-temperature quantum devices.[3–5] The structure and composition of Si_xGe_{1-x} nanowires have great effects on the bandgap values[6] and wave-function distributions,[7] which might induce the electron-hole separation.[8] Ascribed to the intrinsic strain in Si-Ge interface, the bandgap of the core-shell wire is smaller than that of both pure Si and Ge wires with the same diameter.[9] Applied with the axial strain, the valence band offsets of Si_xGe_{1-x} nanowires can be effectively tuned without significantly changing those of conduction band.[10]

Among various possible hydrogen (H) passivated Si_xGe_{1-x} nanowires, it has been reported[8] that the Ge_{core}-Si_{shell} structures are the most stable according to the analysis of formation enthalpy, which indicates Si surface segregation is energetically favorable. For Si_xGe_{1-x} alloys, Ge atoms prefer segregating towards the surface due to the lower surface energy of Ge, verified by both the theoretical simulation and experimental observation.[11,12] However, hydrogen passivants would induce a reversible SiGe site exchange reaction on Ge-terminated Si(001) at temperatures above 250 °C.[13,14] In the presence of chlorine (Cl), Si surface segregation was determined on the Ge-terminated Si/Ge(100) surface through the photoemission spectroscopy, since the Cl–Si–Si–Cl surface is energetically much more stable than the Cl–Ge–Ge–Cl surface.[15] Thus, the passivants play an important role in the stabilities of Si_xGe_{1-x} nanostructures, which can be used for modulating their electronic properties.

For other Si_xGe_{1-x} nanostructures, such as H-passivated nanocrystals, there were significant differences in the electronic and optical properties of Ge-capped Si nanocrystals and Si-capped Ge nanocrystals.[16] There was a low-energy shift of the Photoluminescence (PL) peak experimentally observed from the bandgap of Si nanocrystals to that of Ge nanocrystals with increasing Ge content,[17] and the calculated optical gaps and electron-hole binding energies of H-passivated Si_xGe_{1-x} nanocrystals were found to decrease linearly with x, indicating the sensitivity of optical properties to the Ge content.[18] Grown on the substrate, the equilibrium composition profiles of Si_xGe_{1-x} nanocrystals were found to depend on the slopes and curvatures of surfaces, the presence of corners and edges, the ratio of the strain and chemical mixing energy densities,[19] while the composition profiles during the nonequilibrium growth was dominated by the kinetic growth mode (the layer-by-layer and faceted growth).[20] The

a)E-mail: scxbyang@scut.edu.cn
b)E-mail: xu.h@sustc.edu.cn

electronic and optical properties of Si_xGe_{1-x} nanowires would be substantially influenced by the composition profiles, however, the study of the surface passivants' effect on the composition profiles is still lacking.

In this paper, we have demonstrated that the morphology of Si_xGe_{1-x} nanowires, including the composition profiles, size, and shape, can be effectively modulated by surface passivants. First, we found that there was a strong tendency of Si atoms segregation towards the surface in the X-passivated (X = F, Cl, H) Si_xGe_{1-x} nanowires, and the segregation should be feasible because the Si/Ge exchanging barrier is lower than that of X atoms' desorption. Second, we obtained the composition profiles of Si/Ge distributions by minimizing the Gibbs free energy which is composed of the Si/Ge bond energies and mixing entropy, indicating that the outmost layer of surface should be mostly occupied by Si atoms. Finally, it is found that F-passivated Si_xGe_{1-x} nanowires with certain shape and size would be stabilized at the proper chemical potential of F atoms, where the shape and size of stable nanowires depend on the composition x. We have also investigated the electronic properties of stable F-passivated Si_xGe_{1-x} nanowires.

II. COMPUTATIONAL METHODS

We performed the calculations on the structural stabilities and electronic properties of Si_xGe_{1-x} nanowires, using the density functional theory method implemented in the Vienna *ab initio* simulation package (VASP).[21,22] The projector augmented wave (PAW)[23] and the Perdew-Burke-Ernzerhof GGA (PBE)[24] functionals were employed for the total energies calculations. The cutoff energy was 450 eV and the vacuum distance was set to be 8 Å. With a mesh of $1 \times 1 \times 4$ of k-point grid, all the structures were fully relaxed by the conjugate gradient minimization and the force criteria were 0.01 eV/Å. The k-point grid was increased to $1 \times 1 \times 10$ to obtain accurate energies and band structures with atoms fixed after relaxations. The energy barriers and pathways were obtained using the climbing image nudged elastic band method (CI-NEB).[25]

To study the evolution of composition profiles, we described the Gibbs free energy, $G = E - TS$, by adopting the bond energy model for the total energies (E)[26–28] and considering the mixing entropy (S) of Si/Ge atoms.[20] $S = -k \sum_{i=1}^{N} (x_i ln x_i + (1 - x_i) ln(1 - x_i))$, where x_i is the Si atom occupied ratio of at the ith site. The Gibbs free energy was minimized through the particle swarm optimization (PSO), which was reported to be a practical and efficient method for global optimization.[29]

III. RESULTS AND DISCUSSIONS

We investigate the structural stabilities of X-passivated Si_xGe_{1-x} nanowires with various atomic arrangement of Si and Ge atoms in Sec. III A, as well as the barrier for the passivants' desorption. In Sec. III B, we consider the temperature and passivants' effect on the composition profiles. The stable Si_xGe_{1-x} nanowires with their electronic properties are shown in Sec. III C.

A. First principle calculations

The nanowires we considered is along the ⟨110⟩ direction, with a cross-section of parallelogram. The symbol of $S_{p\times q}$ is used to note the structure with p and q times of basic lattices ($\mathbf{a_1}$,$\mathbf{a_2}$) in the two (110) facets enclosing the wire, where the $S_{3\times3}$ $Si_{0.5}Ge_{0.5}$ nanowire (with the diameter of 1.5 nm) is shown as an example in Fig. 1. With H, F, or Cl passivation, about 20 possible structures were calculated with the random arrangement of Si and Ge atoms for each case. The structures with Ge segregation were found to possess highest total energies, which were set as the reference level. We calculated the energy differences (ΔE) of nanowires compared to the reference level and the ones with lower ΔE are more stable.

As shown in Fig. 1(a), ΔE decreases gradually as the number of Si–X bonds increases. Fitting ΔE with the linear dependence on the ratio of Si–X bonds, we found that the slope was 0.13, 0.85, and 0.35 for H, F, and Cl, respectively. We calculated the bond energies of Si–X and Ge–X bonds and found that the differences are 0.33 eV, 1.20 eV, and 0.61 eV, respectively. Thus, the main contribution of ΔE is from the differences of Si–X and Ge–X bond energies. Note that the nanowire we considered was of small size and the strain energies induced by the mismatch of Si and Ge atoms should be also important. For H-passivated nanowires, the tendency of Si segregation is weak, as the one with complete Si segregation is not the most stable. However, F passivation would induce strong Si segregation, since ΔE decreases significantly with the number of Si–F bonds.

Figure 1(b) shows the potential energy profiles and the structures' evolution for H desorption from SiGe nanowire as a function of reaction coordinates. The bond length's variations of H–H and Si–H exhibit the H atoms desorbing progress where the Si–H bonds breaks and the H_2 molecular forms. Experimentally, H atoms would induce Si segregation at the temperature (T) higher than 600 K, while H atoms would desorb and form H_2 when the temperature is around 800 K.[13] Thus, the exchange barrier of Si and Ge atoms should be lower than that for H atoms' desorption. It is reasonable that the barrier of H desorption was about 2.5 eV in our NEB calculations, since the exchange barrier for Si-Ge atoms was reported to be around 1.5 eV.[30] Note that the barrier of F desorption (about 9 eV, shown in Fig. 1(c)) was much higher than that of H desorption. Thus, Si atoms would segregate to the surface by exchanging with Ge atoms, without F atoms desorption even at higher temperature.

B. Composition profiles

The surface segregation of Si atoms should be feasible because the Si/Ge exchanging barrier is lower than that of passivants' desorption. In the following, we investigate the passivants' effect on the composition profiles, as a function of temperature. As shown in Fig. 1(a), there is an approximately linear dependence of total energies on the number of surface Si atoms. For simplicity, the total energy of structure with j Si atoms on the surface can be estimated to be $-j\alpha$, where α = 0.13, 0.85, and 0.35 eV for the systems with H,

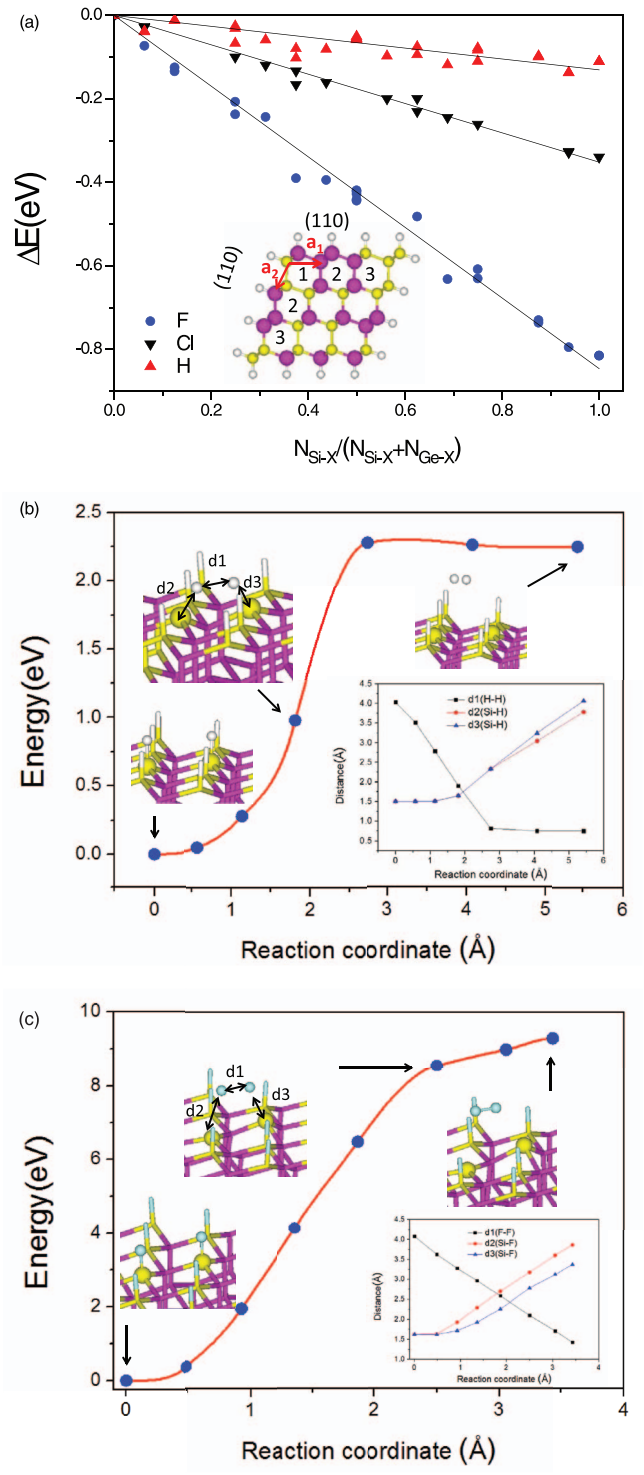

FIG. 1. The differences of total energies of the ⟨110⟩ $Si_{0.5}Ge_{0.5}$ nanowires passivated by X (X = F, Cl, or H) as a function of the configurations. Si/Ge/X atoms are represented by yellow/pink/white balls. Potential energy profiles and transition state structures for (b) H desorption and (c) F desorption from SiGe nanowire. The insets show the bond length's variations of H–H, Si–H, F–F, and Si–F with the reaction coordinates. The nanowire with four unit cells is used in the calculation.

F, and Cl passviants, respectively. Note that the number of total atoms (N) in the unit cell of Si_xGe_{1-x} nanowires $S_{p\times q}$ is $N = 2(p+1)(q+1)$ and the number (Ns) of surface atoms is $Ns = 2(p+q+2)$. Thus, the number f of surface Si atoms under thermal equilibrium was calculated as

$$f = \frac{\sum_{j=0}^{\min(Ns,xN)} j g(j) e^{-j\alpha/kT}}{\sum_{j=0}^{\min(Ns,xN)} g(j) e^{-j\alpha/kT}},$$

where $g(j)$ is the degeneracy factor, i.e., the combination of $\binom{j}{Ns} \times \binom{xN-j}{N-Ns}$.

Figure 2 shows the variations of surface Si atoms ratio as a function of temperature, for X-passivated Si_xGe_{1-x} nanowires ($S_{4\times4}$) (x = 0.125, 0.25, 0.375, and 0.5). There is a maximum of surface Si atoms ratio that indicates the total segregation of Si atoms to the surface at low temperature, while the Si's distribution decreases and becomes uniform on the surface and in the core, as the temperature increases. For example, the max surface Si atom's ratio is 0.5 and 1 for $Si_{0.125}Ge_{0.875}$ and $Si_{0.25}Ge_{0.75}$ nanowires as shown in Figs. 2(a) and 2(b), which gradually decrease to 0.125 and 0.25, respectively. We marked the critical temperature at which the surface Si's ratio is at the mean value of the maximum and minimum. The critical temperature is 725 K, 2174 K, and 5798 K for H, Cl, and F-passivated $Si_{0.125}Ge_{0.875}$ nanowires. Note that the nanowires should be melted at round 1500 K, however, our results emphasized that there was a strongest Si segregation in F-passivated nanowires when the temperature was lower than 1000 K. For $Si_{0.25}Ge_{0.75}$ nanowires, the temperature is 607 K, 1701 K, and 4546 K for H, Cl, and F, respectively. As the Si composition x increases further, the critical temperature increases, indicating the enhancement of Si segregation. It is 843/1011, 2343/2901, and 6263/7778 K for $Si_{0.375}Ge_{0.625}$ and $Si_{0.5}Ge_{0.5}$ nanowires, respectively. Therefore, it could be concluded that Si atoms should be segregated to the surface for F-passivated nanowires at the temperature around 1000 K, in which the Si/Ge exchanging is activated while the nanowires remain stable with the passivants.

To give a detailed figure of composition profiles in the core, we investigated the X-passivated Si_xGe_{1-x} films and minimized the Gibbs free energy with the PSO algorithm.[29] In our previous studies,[26–28] we found that the total energies of group-IV (C/Si) nanostructures could be described by the bond energies of C–C/Si–Si and C–X/Si–X, which has significantly enhanced the efficiency in the determination of structural stabilities. Thus, we used the energies of Si–Si/Si–Ge/Ge–Ge and Si–X/Ge–X bonds to describe the total energies of X-passivated Si_xGe_{1-x} films, focusing on the temperature effect on composition profiles by consider the mixing entropy.

In the Gibbs free energy $G = E - TS$, the total energies were calculated as

$$E = -\sum_{NN}^{core}(x_i x_j E_{Si-Si} + x_i(1-x_j)E_{Si-Ge} + (1-x_i)x_j E_{Si-Ge} + x_i x_j E_{Ge-Ge}) - \sum^{surface}(x_i E_{Si-X} + (1-x_j)E_{Ge-X}),$$

where the bond energies of E_{Si-Ge}, E_{Si-Si}, and E_{Ge-Ge} were calculated to be 2.05 eV, 2.27 eV, and 1.84 eV, E_{Si-X} and

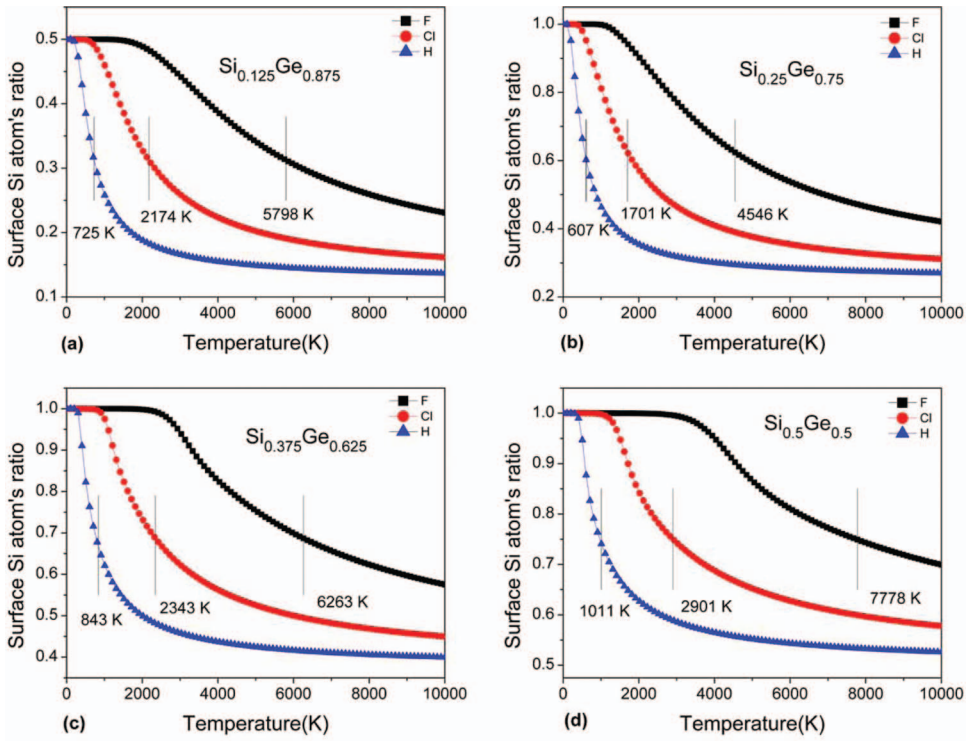

FIG. 2. The variations of surface Si atoms ratio as a function of temperature, for X-passivated Si_xGe_{1-x} nanowires: (a) $Si_{0.125}Ge_{0.875}$; (b) $Si_{0.25}Ge_{0.75}$; (c) $Si_{0.375}Ge_{0.625}$; (d) $Si_{0.5}Ge_{0.5}$. The black squares/red circles/blue triangles indicate the passivants of F, Cl, and H, respectively.

E_{Ge-X} were the bond energies between Si/Ge atoms and passivants. The first sum runs over all the nearest-neighbor atom pairs in the core, the second sum runs over all atoms on the surface, and x_i, x_j is the Si atom occupied ratio of at the i, jth site. The mixing entropy of Si/Ge atoms[20] was calculated as $S = -k\sum_{i=1}^{N}(x_i \ln x_i + (1-x_i)\ln(1-x_i))$.

We considered a X-passivated (111) $Si_{0.5}Ge_{0.5}$ films with the thickness of 26 Å and showed the distributions of x_i as a function of temperature in Fig. 3. Layers 1–8 indicate atomic layers from the outmost one to the ones in the core, with increasing distances to the surface. For both F- and H-passivated films, the oscillations of Si atom's ratio are more significant

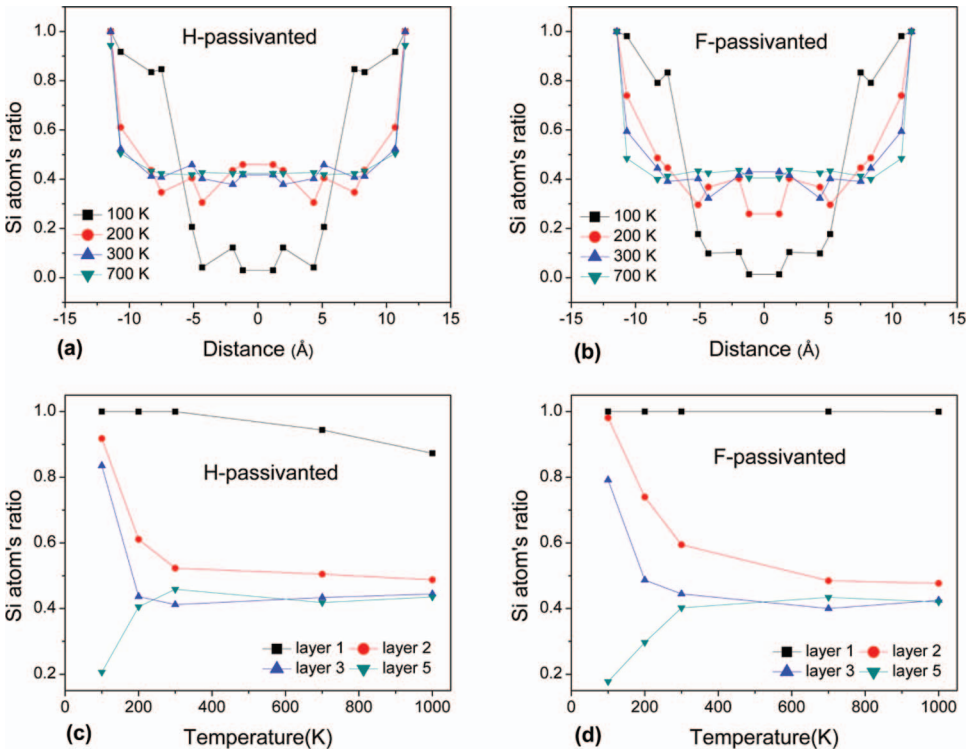

FIG. 3. The distributions of Si ratio in a $Si_{0.5}Ge_{0.5}$ films as a function of temperature: (a) with H passivants; (b) with F passivants. The Si ratio of the layer 1, 2, 3, 5 as a function of temperature and passivants are shown in (c) and (d).

at low temperature than that at high temperature. Note that F passivation would induce a stronger Si surface segregation compared to H passivation. As shown in Fig. 3(c) and 3(d), the Si atom's ratio on the layer 1 varies from 1 to 0.8 as the temperature increases for H-passivation, while the Si atom's ratio with F-passivation remain 1 for T = 100–1000 K. For layers 2–4, the Si atom's ratio gradually decreases from the maximum and approach 0.5, while it gradually increases from the minimum and approach 0.5 for layers 5–8. Thus, there is an even mixing of Si and Ge atoms for layers 2–8 at the temperature of 1000 K, while the outmost layer is mostly occupied by Si atoms due to the passivants' effect.

C. Stable nanowires and electronic properties

As verified above, the composition profiles would evolve with the temperature and the kinds of passivants. However, the outmost surface layer should be occupied by Si at large temperature regions for F-passivated Si_xGe_{1-x} nanowires. In the following, we focused on the passivants' effect on the structural stabilities and electronic properties of F-passivated ⟨110⟩ Si_xGe_{1-x} nanowires.

To determine the stabilities of F-passivated ⟨110⟩ Si_xGe_{1-x} nanowires, we defined the formation energies of $Si_{mx}Ge_{m(1-x)}F_n$ as

$$E_f = (E_{tot}(\mathrm{Si}_{mx}\mathrm{Ge}_{m(1-x)}\mathrm{F}_n) - n\mu_\mathrm{F} - m(x\mu_\mathrm{Si} + (1-x)\mu_\mathrm{Ge}))/m,$$

where $E_{tot}(\mathrm{Si}_{mx}\mathrm{Ge}_{m(1-x)}\mathrm{F}_n)$ and $\mu_\mathrm{F}/\mu_\mathrm{Si}/\mu_\mathrm{Ge}$ are the total energies of the nanowires and the chemical potential of F/Si/Ge atoms, respectively. In our calculations, μ_Si and μ_Ge are the total energies of isolated Si and Ge atoms. μ_F is the chemical potential of F atoms in the gas phase of F_2 at given pressure and temperature.

We considered the possible structures of $S_{p\times q}$, where p = 1–3 and q = 1–15. Si segregation are energetically preferable and the nanowires are constructed with as many Si-F bonds as possible. The formation energies (E_f) of $Si_{0.5m}Ge_{0.5m}F_n$ are calculated as $E_f = (E_{tot}(\mathrm{Si}_{0.5m}\mathrm{Ge}_{0.5m}\mathrm{F}_n) - n\mu_\mathrm{F} - 0.5m(\mu_\mathrm{Si} + \mu_\mathrm{Ge}))/m$.

Figure 4(a) shows a variation of the stable structures with a change of chemical potential of F atoms, where the formation energies of all the nanowires increase as μ_F increases. We also consider the SiGe bulk structure and the SiF_4/GeF_4 molecules (1:1 mixed) for comparison. For μ_F lower than −3.55 eV, the SiGe bulk structure is the most stable, while the SiF_4/GeF_4 molecules are energetically favored for μ_F higher than −3.39 eV. It is reasonable that F atoms prefer to desorb in the F-poor environment and fluorinate all the Si and Ge atoms in the F-rich condition. Note that the $S_{3\times2}$ nanowire is the most stable among these nanowires in the interval of $\mu_\mathrm{F} \in [-3.55, -3.39]$eV, prevailing the bulk structure and mixed molecules.

Focusing on the stability evolution, we calculated the formation energies of all structures at $\mu_\mathrm{F} = -3.4$ eV. As shown in Fig. 4(b), the most stable structure is $S_{3\times2}$, which corresponds to the local minima of formation energies in the series of $S_{p\times2}$ and $S_{p\times3}$. Note that $p = 3$ corresponds to the local minima of formation energies for the nanowires with the cross-section

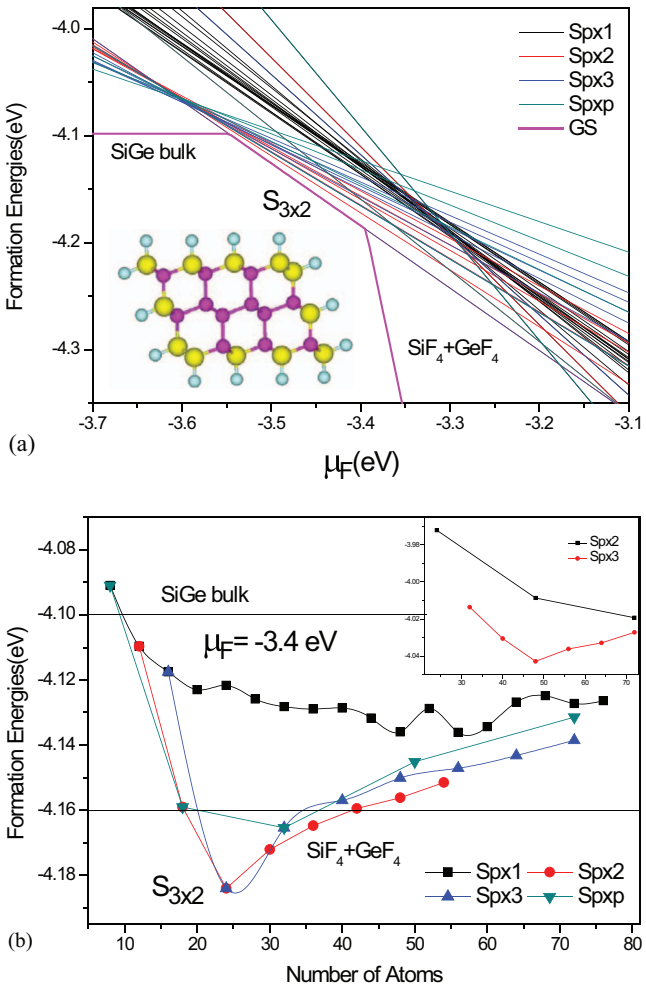

FIG. 4. Stabilities of the ⟨110⟩ $Si_{0.5}Ge_{0.5}$ nanowires of various shape and diameter. (a) phase diagram of ground states for various μ_F; (b) the formation energies at $\mu_\mathrm{F} = -3.4$ eV, with the energies of SiGe bulk and corresponding SiF_4/GeF_4 molecules shown in blue and black lines, respectively.

of rhombus ($S_{p\times p}$), which is less stable than the $S_{3\times2}$ structure. The formation energies of SiGe bulk structure and the SiF_4/GeF_4 molecules are also shown for comparison, which are both higher than that of the $S_{3\times2}$ structure. For the series of $S_{p\times1}$, the formation energies are relative higher, though decreasing as the Si/Ge number increases with small fluctuations. Therefore, the nanowire is the most stable among these nanowires at $\mu_\mathrm{F} = -3.4$ eV.

To demonstrate the effect of Si/Ge composition x, we also investigated the ⟨110⟩ $Si_{0.375}Ge_{0.625}$ nanowires for comparison, considering the structures of the $S_{p\times2}$ and $S_{p\times3}$ series. Similarly, $S_{4\times3}$ corresponds to the local minima of formation energies at $\mu_\mathrm{F} = -3.4$ eV, as shown in the inset of Fig. 4(b). According to the phase diagram (not shown), we found that the $S_{4\times3}$ wire should be the most stable one in the interval of $\mu_\mathrm{F} \in [-3.45, -3.27]$eV, prevailing the bulk structure and mixed molecules with the composition of Si_3Ge_5. Thus, the chemical composition x plays an important role in modifying the stabilities of Si_xGe_{1-x} nanowires, including the shape and diameter.

In core-shell Ge/Si nanowires, the local and global geometry and electronic structure revealed the strong core-type

specific features for both structural and electronic properties,[31] due to the difference between Ge–Ge and Si–Si bonds. Based on analytical effective-mass model predictions and first-principles calculations, the charge separation in Ge-core valence states conduction states was clarified, in good agreement with experimental observations of accumulation of a Ge-core hole gas in core-shell nanowires.[32] The type-I band alignment in Ge/Si nanowires, i.e., the charge densities of conduction bands edge (CBE) and valence band edge (VBE) mostly appears in Ge core atoms, which would enable both *n*-type and *p*-type quantum-well transistors to be fabricated using Ge/Si nanowires for high-speed logic applications. Recently, it has been reported[33] that the type-I transition of Ge/Si nanowires can be achievable due to the quantum confinement when ⟨100⟩ and ⟨111⟩ nanowires are fabricated in nanometer scale, however, the extra axial lattice strain would be required for the ⟨110⟩ nanowires to induce the type-I/II band alignment transition. Figure 5 shows the electronic properties of $S_{3\times2}$ and $S_{4\times3}$, the two stable Si/Ge nanowires, including their band structures and the charge distribution of CBE and VBE. Both the wires are of direct bandgap, with the value of 0.89 and 0.67 eV, respectively. As shown in Fig. 5(a), the charge distribution of VBE and CBE concentrate in the core for the $S_{3\times2}$ wire, indicating the representative type-I band alignment. For the $S_{4\times3}$ wire, the charge of VBE mainly distributes in the core, while the charge distribution of CBE is near the surface. However, the type-I band alignment should be preserved since most charges of VBE and CBE still distribute at Ge atoms. Thus, modulating the shape and diameter of nanowires with the control of chemical composition and the passivants can be used for the tuning of electronic properties and design of optoelectronic nano-device.

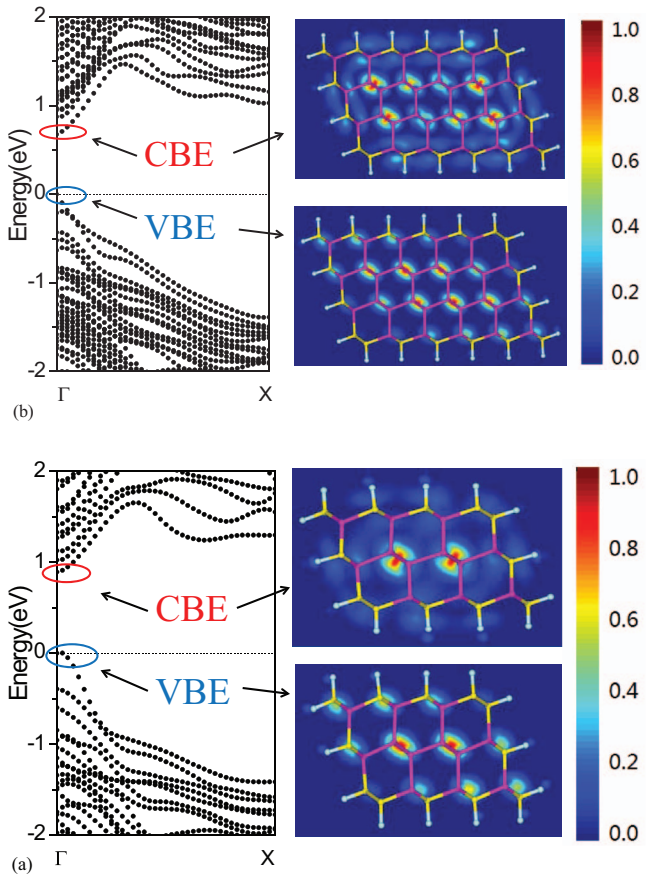

FIG. 5. Band structures and charge distributions of CBE and VBE of the stable Si_xGe_{1-x} nanowires passivated by F atoms: (a) $Si_{0.5}Ge_{0.5}$; (b) $Si_{0.375}Ge_{0.625}$. All the valence bands maximums are shifted to zero.

IV. CONCLUSION

In summary, we have shown that Si atoms preferred to segregate towards the surface due to the strong Si–X bonds (X = F, Cl, H) in X-passivated Si_xGe_{1-x} nanowires. The Si surface segregation should be feasible because the Si/Ge exchanging barrier is lower than that of passivants' desorption, and Si atoms should be stabilized at the outmost surface layer even at round 1000 K according to the composition profiles. With total segregations of Si atoms, the stable structures of F-passivated Si_xGe_{1-x} nanowires depend on the composition x and the chemical potential of F atoms. Our finding indicates that the electronic properties of Si_xGe_{1-x} nanowires can be tuned by modulating the shape and diameter of nanowires with the control of chemical composition and the passivants, providing a practical avenue for the design of optoelectronic nano-device.

ACKNOWLEDGMENTS

This work was supported by NSFC (Grant Nos. 11104080 and 11204185), the Fundamental Research Funds for the Central Universities (Grant No. 2013ZZ0082), and Guangdong Natural Science Foundation (S2011040005430). The computing resources from the HPC Lab, Shenzhen Institute of Advanced Technology, Chinese Academy of Sciences (CAS), National Supercomputing Center in Shenzhen (NSCCSZ), and from ScGrid of the Supercomputing Center, Computer Network Information Center of CAS, are gratefully acknowledged.

[1]M. d'Avezac, J.-W. Luo, T. Chanier, and A. Zunger, Phys. Rev. Lett. **108**, 027401 (2012).
[2]L. J. Lauhon, M. S. Gudiksen, D. Wang, and C. M. Lieber, Nature (London) **420**, 57 (2002).
[3]W. Lu, J. Xiang, B. P. Timko, Y. Wu, and C. M. Lieber, Proc. Natl. Acad. Sci. U.S.A. **102**, 10046 (2005).
[4]L. Hu and G. Chen, Nano Lett. **7**, 3249 (2007).
[5]Y. Hu, H. O. H. Churchill, D. J. Reilly, J. Xiang, C. M. Lieber, and C. M. Marcus, Nat. Nanotechnol. **2**, 622 (2007).
[6]J. Yang, C. Jin, C. Kim, and M. Jo, Nano Lett. **6**, 2679 (2006).
[7]D. B. Migas and V. E. Borisenko, Phys. Rev. B **76**, 035440 (2007).
[8]M. Amato, M. Palummo, and S. Ossicini, Phys. Rev. B **80**, 235333 (2009).
[9]X. Peng and P. Logan, Appl. Phys. Lett. **96**, 143119 (2010).
[10]S. Huang and L. Yang, Appl. Phys. Lett. **98**, 093114 (2011).
[11]P. C. Kelires and J. Tersoff, Phys. Rev. Lett. **63**, 1164 (1989).
[12]N. Ikarashi, K. Akimoto, and T. Tatsumi, Phys. Rev. Lett. **72**, 3198 (1994).
[13]E. Rudkevich, F. Liu, D. E. Savage, T. F. Kuech, L. McCaughan, and M. G. Lagally, Phys. Rev. Lett. **81**, 3467 (1998).
[14]S.-J. Kahng, Y. H. Ha, D. W. Moon, and Y. Kuk, Appl. Phys. Lett. **77**, 981 (2000).
[15]D. S. Lin, S. Y. Pan, and M. W. Wu, Phys. Rev. B **64**, 233302 (2001)).
[16]L. E. Ramos, J. Furthmüller, and F. Bechstedt, Phys. Rev. B **72**, 045351 (2005).
[17]S. Takeoka, K. Toshikiyo, M. Fujii, S. Hayashi, and K. Yamamoto, Phys. Rev. B **61**, 15988 (2000).

[18]E. L. de Oliveira, E. L. Albuquerque, J. S. de Sousa, and G. A. Farias, J. Appl. Phys. **103**, 103716 (2008).
[19]N. V. Medhekar, V. Hegadekatte, and V. B. Shenoy, Phys. Rev. Lett. **100**, 106104 (2008).
[20]X. B. Niu, G. B. Stringfellow, and Feng Liu, Phys. Rev. Lett. **107**, 076101 (2011)
[21]G. Kresse and J. Furthmüller, Phys. Rev. B **54**, 11169 (1996).
[22]G. Kresse and D. Joubert, Phys. Rev. B **59**, 1758 (1999).
[23]P. E. Blöchl, Phys. Rev. B **50**, 17953 (1994).
[24]J. P. Perdew, K. Burke, and M. Ernzerhof, Phys. Rev. Lett. **77**, 3865 (1996).
[25]G. Henkelman, B. P. Uberuaga, and H. Jónsson, J. Chem. Phys. **113**, 9901 (2000).
[26]H. Xu, X. B. Yang, C. S. Guo, and R. Q. Zhang, Appl. Phys. Lett. **95**, 253106 (2009).
[27]X. B. Yang, Y. J. Zhao, H. Xu, and B. I. Yakobson, Phys. Rev. B **83**, 205314 (2011).
[28]H. Lu, Y. J. Zhao, X. B. Yang, and H. Xu, Phys. Rev. B **86**, 085440 (2012).
[29]J. Kennedy and R. Eberhart, *Particle Swarm Optimization* (IEEE, Piscataway, NJ, 1995), p. 1942.
[30]P. Bogusławski and J. Bernholc, Phys. Rev. Lett. **88**, 166101 (2002).
[31]R. N. Musin and X. Q. Wang, Phys. Rev. B **71**, 155318 (2005).
[32]A. Nduwimana, R. N. Musin, A. M. Smith, and X. Q. Wang, Nano Lett. **8**, 3341 (2008).
[33]J. Kim, J. H. Lee, and K. H. Hong, J. Phys. Chem. Lett. **4**, 121 (2013).